

**ICSO 2016**

**International Conference on Space Optics**

Biarritz, France

18–21 October 2016

*Edited by Bruno Cugny, Nikos Karafolas and Zoran Sodnik*



***Transportable system for in-field testing of adaptive optical pre-compensation for optical feeder links***

*R. Berlich*

*T. Kopf*

*A. Brady*

*N. Leonhard*

*et al.*



International Conference on Space Optics — ICSO 2016, edited by Bruno Cugny, Nikos Karafolas, Zoran Sodnik, Proc. of SPIE Vol. 10562, 105625V · © 2016 ESA and CNES  
CCC code: 0277-786X/17/\$18 · doi: 10.1117/12.2296206

## TRANSPORTABLE SYSTEM FOR IN-FIELD TESTING OF ADAPTIVE OPTICAL PRE-COMPENSATION FOR OPTICAL FEEDER LINKS

R. Berlich<sup>1</sup>, T. Kopf<sup>1</sup>, A. Brady<sup>1</sup>, N. Leonhard<sup>1</sup>, A. Kamm<sup>1</sup>, C. Reinlein<sup>1</sup>

<sup>1</sup>Fraunhofer Institute for Applied Optics and Precision Engineering, Albert-Einstein-Straße 7, 07745 Jena, Germany

### I. INTRODUCTION

Pre-compensation of atmospheric wavefront distortions using adaptive optics (AO) provides a promising approach for stabilizing optical feeder links in Earth-to-space laser communication applications. The general concept is based on the utilization of an optical signal from the target in space, i.e. the downlink communication laser signal of the satellite, in order to measure the aberrated wavefront after passing through the atmosphere. Subsequently, this information is used to pre-distort the uplink laser signal of the ground station before passing through the atmosphere in order to compensate for the introduced aberrations. So far, this method has only been studied in a laboratory environment [1], which necessitates a simplified implementation of atmospheric turbulences using a thin diffractive optical element. In this paper, we present the development of a transportable, adaptive optical system, which, allows for an in-field assessment of this approach under real atmospheric turbulence conditions. In addition, the system architecture is capable of investigating the influence of different beam paths between the uplink and downlink signal. This aspect is of particular importance for Earth-to-space communication scenarios, where a pre-defined point-ahead angle needs to be taken into account.

### II. SYSTEM CONCEPT OVERVIEW

In order to demonstrate the feasibility of the pre-compensation approach in-field, our approach is to implement a horizontal laser link at 1064nm over an extended, on-ground distance of several hundred meters. The basic system concept is shown schematically in Fig. 1. The setup comprises two main subsystems that represent the space terminal breadboard (GTB) and the ground terminal breadboard (STB), respectively. The former provides a circular polarized beacon signal provided by the downlink laser, which propagates through the turbulent atmosphere and illuminates an emitting telescope attached to the GTB. This telescope is used to initially couple the downlink signal into an adaptive optics setup inside the GTB. The wavefront distortions are measured using a customized Shack-Hartmann sensor. The obtained information is used in a real time, adaptive optics control loop to post-compensate the downlink signal using a tip/tilt and a deformable mirror. At the same time, an uplink laser beam is coupled into the AO setup, where a tailored wavefront tilt is applied in order to adjust its point-ahead-angle. The beam subsequently passes through the optical system in the reverse direction compared to the downlink beam and the wavefront is pre-distorted by the tip/tilt and a deformable mirror. In order to minimize optical crosstalk, i.e. straylight from the uplink laser that potentially falls onto the downlink wavefront sensor, both beams are separated inside the GTB by selecting different linear polarization states in the horizontal and vertical directions, respectively. When the uplink laser is coupled into the emitting telescope, a quarter-wave-plate is incorporated to circularly polarize the emitted beam. After propagation to the STB and passing through the atmosphere, the residual beam spreading and wandering of the uplink beam is measured inside the uplink analysis part of the STB in order to quantify the efficiency of the pre-compensation.

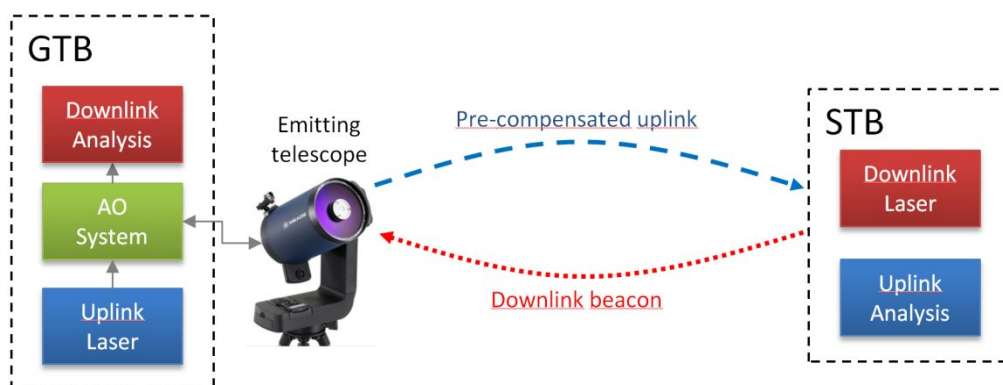


**Fig. 1.** Basic concept of investigating the laser pre-compensation approach based on an optical link between the ground terminal breadboard (GTB) and the space terminal breadboard (STB)

### III. OPTICAL DESIGN AND MODELLING

#### A. Beam diameter optimization

The most essential elements of the AO system inside the GTB that determine its overall size include the deformable mirror (DM), the tip/tilt mirror (TTM) and the wavefront sensor (WFS). Before the actual optical design can be developed, the required beam size at these individual elements needs to be determined. Since the AO control loop is based on the real-time FPGA based system developed in [1,2], the beam diameter at the wavefront sensor is already dictated. Furthermore, the tip/tilt mirror as applied in [2] is incorporated, which pre-determines the respective beam size as well. The AO system utilizes a unimorph deformable mirror manufactured at Fraunhofer IOF. It allows for a large beam diameter of up to 50 mm, which is particularly advantageous for prospective applications that require incorporating up to 30 - 50 lasers beams simultaneously with a respective power of approximately 30 W. To this end, it features a customized coating in order to minimize temperature-induced deformations. The design of the mirror actuator layout, which is illustrated in Fig. 2 a), is predetermined by existing DM modules. However, the actual diameter  $D$  that is illuminated by the uplink as well as the downlink beam remains a variable of the optical design. In order to optimize this beam diameter, the performance of the wavefront correction is theoretically assessed under different turbulence conditions based on a customized numerical simulation tool. In particular, the tool initially creates a large number of randomly distorted atmospheric wavefronts that follow Kolmogorov turbulence theory. These phase screens feature a tailored average Fried parameter  $r_0$ , which is selected in the order of 7 times the diameter  $D$ , representing strong turbulence conditions. Subsequently, the tip and tilt contributions of the wavefronts are subtracted, since they will be controlled for separately by the TTM. Based on the simulated influence function of the DMs actuators, the tool calculates the required voltages that need to be applied to compensate for these wavefronts by means of a least square fitting. These voltages represent an important figure of merit to determine the optimum beam diameter  $D$ . Small average voltages ease the requirements for the voltage supply and furthermore benefit the control loop frequency. The second figure of merit is provided by the obtained Strehl ratio of the residual wavefront after the DM correction. In order to optimize these two figures, an iterative calculation loop, which performs this simulation for a varying diameter  $D$ , is conducted. The corresponding results are shown in Fig. 2 b). As can be seen, the average voltage that must be applied to the DM actuators is decreasing with larger diameters  $D$  and eventually saturates at around 35 V. In contrast, the quality of the correction is deteriorating and the Strehl ratio is decreasing. Accordingly, an optimum beam diameter of approximately 31mm can be identified under the aforementioned conditions.

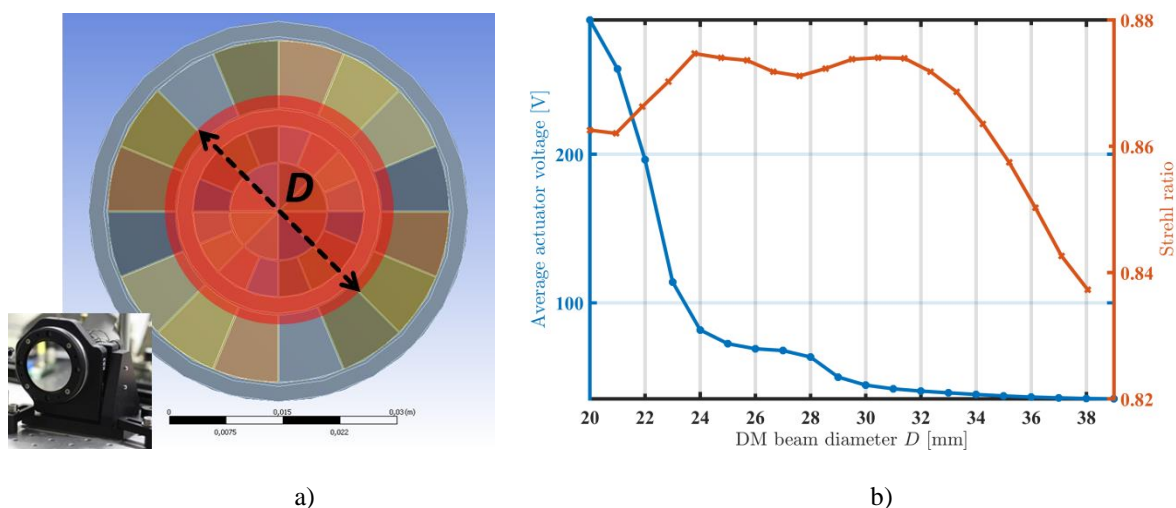


**Fig. 2.** a) Image of mounted deformable mirror and schematic actuator layout. The illustrated red, circular area of diameter  $D$  indicates the incident beam extension, which is optimized based on a customized numerical simulation tool. b) Simulated dependency of the average required actuator voltage and achieved Strehl ratio on the beam diameter  $D$  under strong turbulence conditions.

#### B. Ground terminal optical design

After the beam diameters at the individual AO elements are fixed, the optical system of the GTB can be designed. The final layout of the design is shown in Fig. 3. The optical interface between the emitting telescope and the GTB is established by a physical aperture stop that defines the entrance pupil (EP) of GTB. Therefore, the breadboard can potentially be attached to a variety of different emitting telescopes. The respective telescope pupil

simply needs to be projected onto the GTB pupil using two folding mirrors for line of sight adjustments and an adequate collimating lens with a matching F-number. Note that an additional quarter wave plate (QWP) needs to be placed in the optical path between the telescope and the GTB in order to convert the incoming circularly polarized downlink beam into linear polarized light in the horizontal direction. Within the GTB optical design, multiple telescope assemblies successively image the downlink wavefront at the entrance pupil onto TTM, the DM and the Shack-Hartmann WFS, while ensuring the proper beam diameters. An adjustable beam splitting cube is placed in front of the WFS and the respective collimating lens. The additional beam path allows for either placing a camera to monitor the PSF distribution or a fiber input in the downlink laser focus for additional analysis.

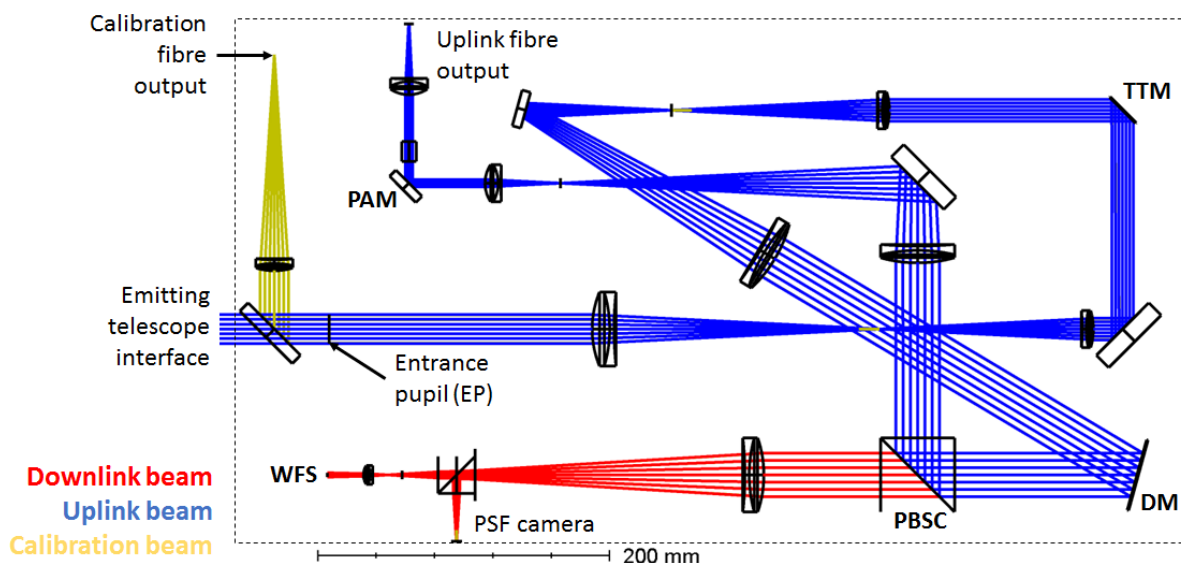


**Fig. 3.** Optical design of the ground terminal breadboard (GTB) illustrating the downlink, uplink and calibration channel.

The uplink beam is coupled into the GTB using a collimating lens and a point-ahead-mirror (PAM). An additional telescope and a polarizing beam splitter cube are utilized to project the uplink wavefront at the PAM onto the DM. The uplink beam inside the AO setup is thus linearly polarized in the vertical direction. Accordingly, the uplink and the downlink channel are separated by their respective polarization directions, and potential straylight from the uplink source, i.e. ghost images, that could fall onto the downlink WFS is minimized.

The optical design is based exclusively on commercially available lenses, i.e. achromatic doublets optimized for a wavelength range of 1050 to 1700 nm, in order to minimize the costs and development time of the setup. The respective F-numbers of the lenses are selected based on a trade-off between a diffraction limited performance and a minimized overall system length. In fact, the achromatic design in combination with broadband antireflection coatings potentially allow for operating the GTB at higher wavelengths, i.e. around 1550nm (terrestrial fiber telecommunication wavelength), considering only minor adjustments. In addition to the actual telescope lenses, multiple folding mirrors are incorporated in order to optimize the overall layout with regard to supplementary design goals. First, they enable to facilitate a high compactness of the breadboard. Furthermore, all elements that need to be accessed by external wiring, such as the WFS, TTM, DM as well as the fibre outputs, are beneficially located around the border of the GTB. Finally, the optical interface to the emitting telescope is close to the GTB's center of gravity along the longer axis, which benefits the mechanical mounting on top of the emitting telescope.

As can be seen in Fig. 3, the optical setup features a calibration laser that is coupled into the AO system using a beam splitter in front of the entrance pupil. It is used for aligning the opto-mechanical elements, calibrating the wavefront sensor and PSF camera as well as measuring the actuator influence function of the DM and the TTM. Furthermore, it can be utilized as a reference signal to co-align the GTB with the emitting telescope.

### C. Space terminal optical design

The optical design of the space terminal breadboard is shown in Fig. 4. The uplink beam enters the STB through an initial quarter wave plate, which converts it into linear polarized light in the horizontal direction in order to pass the subsequent PBSC. Note that the aperture of the respective elements is significantly oversized with regard to the incoming beam diameter. Thus, the uplink beam profile can be acquired for point-ahead angles that span

multiple isoplanatic angles without needing to translate the STB. The following telescope demagnifies the incoming beam before it is imaged by a fast camera detector. The recorded uplink PSF distribution can be used to quantify the quality of the pre-compensation and the influence of the PAA.

Finally, Fig. 4 shows the fibre output of the downlink beacon, which is collimated and polarized using a commercially available fibre collimator and polarizer. The respective divergence angle is adapted to ensure that ground terminal is completely illuminated, even under strong atmospheric turbulences.

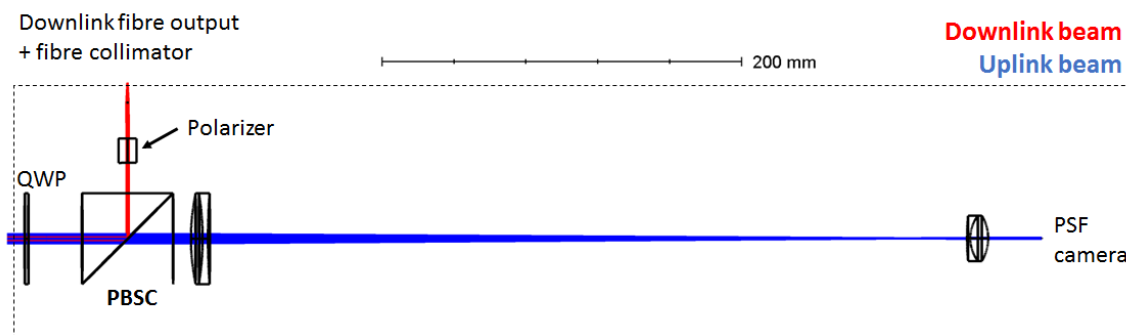


Fig. 4. Optical design of space terminal breadboard (STB).

#### IV. GROUND TERMINAL BREADBOARD IMPLEMENTATION

After finalizing the optical design of the GTB, the mechanical concept is developed. Due to the compact optical design, the entire opto-mechanical system is implemented on a single, commercially available breadboard with a size of only 75cm x 45cm. Commercial lens holders with translation capabilities in x- and y-direction mount the individual optical elements. In combination with an optical rail system, accurate alignment in all three translation axes can be performed, while ensuring minimum angular misalignments.

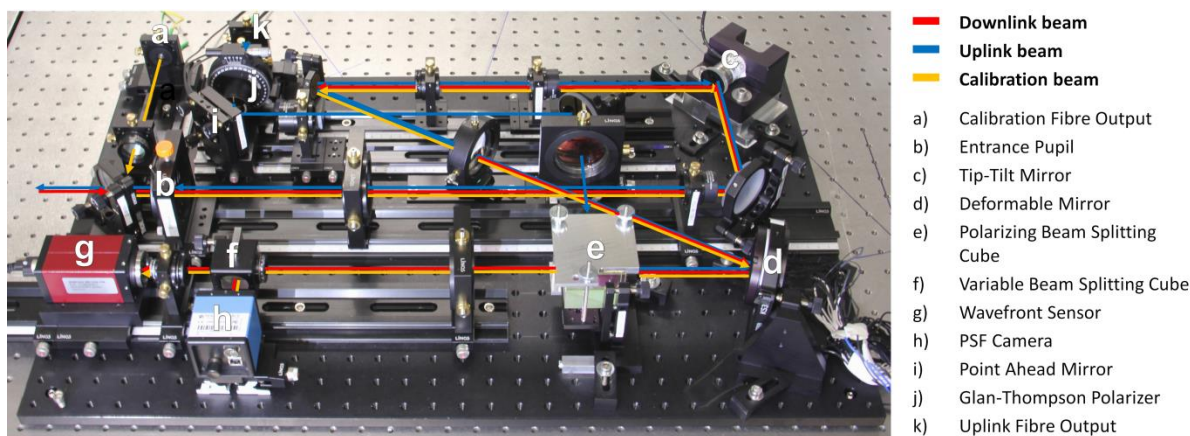
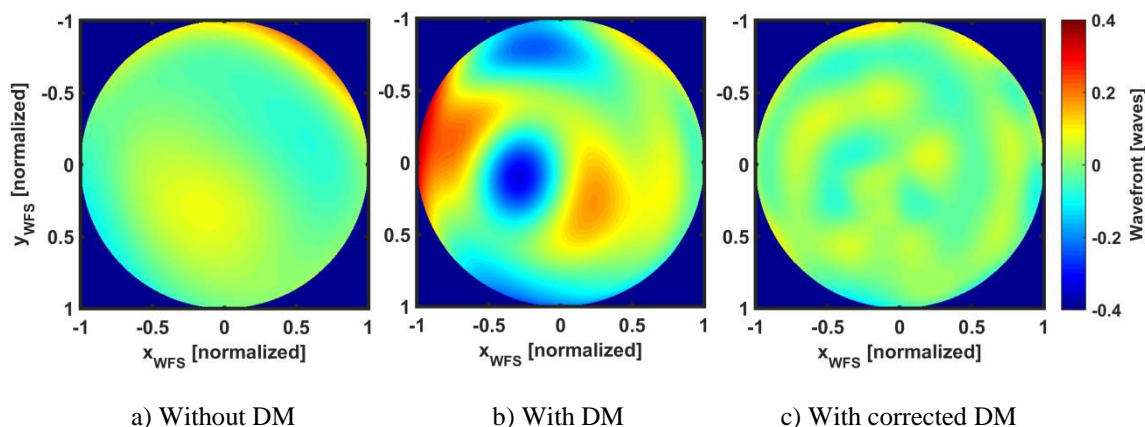


Fig. 5. Image of implemented ground terminal breadboard. The respective beam paths are indicated and the main elements are referenced. Note that the commercial WFS, which was used for alignment and characterization, is shown and the final customized WFS still needs to be implemented

The collimated calibration laser beam is initially used to successively setup up all opto-mechanical components of the downlink as well as the uplink channel. Hereby, the physical entrance pupil provides a fixed global reference plane. Each of the following telescope lens assemblies is aligned according to two boundary conditions. On the one hand, a collimated wavefront with minimized aberrations is obtained by adjusting the separation of the two respective lenses using a commercial wavefront sensor. On the other hand, their absolute axial position is aligned in order to ensure that the entrance pupil, TTM, DM, WFS as well as the PAM are located at conjugated planes. Additional iris apertures are added at different beam focus locations, which mitigates straylight by blocking residual ghost images. It should be pointed out that the setup is initially aligned using a static mirror at the location of the DM in order to avoid wavefront distortions of the uncontrolled actuators that could degrade the alignment accuracy. The finalized ground terminal breadboard setup, including the deformable mirror, is shown in Fig. 5.

Note that the image still shows the alignment wavefront sensor, which will eventually be replaced by the customized WFS developed in [1].

After the final alignment of all opto-mechanical compents, the wavefront of the calibration beam is measured at the final WFS location. The obtained result is shown in Fig. 6 a), which demonstrates the diffraction limited performance of the setup. The residual aberrations (excluding tip/tilt errors) lead to a RMS wavefront error as low as 52 nm at 1064 nm wavelength. Fig. 6 b) provides the wavefront distribution after the deformable mirror is implemented, which initially results in an increased RMS error of approximately 125 nm. However, these static wavefront distortions can be corrected as soon as the AO control loop is implmented, which will be the next step of the developments. In order to assess the final, corrected wavefront error of the system, the AO correction is simulated according to the beam diameter optimization approach described in the previous chapter. The resulting diffraction limited wavefront shown in Fig. 6 c) is subject to a residual RMS wavefront error of 40 nm. Finally, an equivalent wavefront characterization was performed for the uplink channel of the GTB and the comparable results were obtained.



**Fig. 6.** Measured wavefront distribution of the calibration laser inside the GTB, a) without and b) with the implemented deformable mirror. c) Simulated wavefront of GTB after correction by the AO control loop.

## V. CONCLUSIONS AND OUTLOOK

In conclusion, the development status of a transportable, adaptive optical system, which allows for an in-field assessment of a laser pre-compensation approach under real atmospheric turbulence conditions was presented. The optical design of the two respective subsystems was described, including the optimization of the beam diameter at the deformable mirror. The opto-mechanical implementation of the compact ground terminal breadboard was depicted, and initial wavefront measurement results that demonstrate the diffraction limited performance of the GTB system were provided.

In the next step of the development, laboratory tests the AO control loop will be performed based on artificial turbulences provided by a rotating phase screen. Subsequently, the developed GTB will be mounted on a 30 cm Newton type telescope and initial tests of the laser link will be performed in the laboratory. Finally, we will perform in-field tests over an extended, on-ground distance of 700 m under real atmospheric turbulence conditions and investigate the dependency of the pre-compensation efficiency on the point ahead angle.

## ACKNOWLEDGMENT

The funding support of the Bundesministerium für Wirtschaft und Energie and the respective project management agency DLR Raumfahrtmanagement is gratefully acknowledged. This work is funded under contract number 50YB1628.

## REFERENCES

- [1] N. Leonhard R. Berlich, S. Minardi, A. Barth, S. Mauch, J. Mocci, M. Goy, M. Appelfelder, E. Beckert, and C. Reinlein "Real-time adaptive optics testbed to investigate point-ahead angle in pre-compensation of Earth-to-GEO optical communication", *Opt. Expr.*, vol. 24, pp. 13158-13172, 2016.
- [2] S. Mauch, A. Barth, J. Reger, C. Reinlein, M. Appelfelder, and E. Beckert, "FPGA-accelerated adaptive optics wavefront control part II," *Proc. SPIE* 9343, 93430Y, 2015.